Původní práce

POLYTYPISM OF PYROPHYLLITE AND TALC

Part I. OD interpretation and MDO polytypes

SLAVOMIL ĎUROVIČ, ZDENĚK WEISS*)

*Institute of Inorganic Chemistry, Centre of Chemical Research,
Slovak Academy of Sciences, Dúbravská cesta 5, 842 36 Bratislava
) Coat Research Institute, 716 07 Ostrava-Radvanice

Received 26. 4. 1982

Polytypic crystal structures of pyrophyllite and talc with idealized symmetry of their tetrahedral sheets are OD structures consisting of two kinds of layers and belonging to category I. This explains the polytypism of these minerals from the point of view of their symmetry and facilitates the derivation of their standard (MDO) polytypes which are needed for establishing identification criteria. There are 30 non-congruent (22 non-equivalent) MDO polytypes within the pyrophyllite family and 12 (10) MDO polytypes within the talc family. The ideal ditrigonalization of tetrahedral sheets leaves the number of MDO polytypes unchanged, but reduces the stacking possibilities of individual OD layers and causes individual polytypes to appear as members of either of two crystallochemically independent subfamilies within the corresponding pyrophyllite or talc family. Individual polytypes are characterized by fully descriptive symbols which fit into a unified symbolism of polytypes of sheet silicates.

INTRODUCTION

This paper presents the treatment of polytypism in the pyrophyllite and talc family from the point of view of the theory of OD structures (Dornberger—Schiff, [1]—[4]). It is a part of a general project dealing with the polytypism of sheet silicates and follows the studies of kaolinite-type structures [5], [6], micas [7], Mg-vermiculite [8] and chlorites [9], [10]. The goal of these studies is to work out a unified geometric theory of polytypism of sheet silicates which could bring a better understanding into this complex matter and to establish classification and identification criteria for polytypes of these substances.

The results of this paper are based on structural studies of pyrophyllite and talc [11]—[19]. The structures of polytypes of these minerals are closely related to those of micas. Since the OD interpretation of micas has been described in [7], this contribution will make use of basic terms, definitions, polytype symbolism as well as some fundamental considerations introduced there and the reader is asked to consult the paper on micas prior to the study of this paper.

OD INTERPRETATION OF THE IDEALIZED MODEL OF PYROPHYLLITE AND TALC STRUCTURES

In any structure within the pyrophyllite or talc family there are — in contrast to micas — no planes of interlayer cations between adjacent silicate sheets of neighbouring 2 : 1 layers. Accordingly, there is no "anchoring effect" fixing these

two sheets firmly together, thus the sheets do not belong to one nonpolar OD layer any more and they have to be considered as belonging to two separate polar OD layers. Taking the symmetry of tetrahedral sheets in first approximation as hexagonal, we arrive at the following choice of OD layers for which the structure of any pyrophyllite or talc polytype can be considered as OD structure consisting of two kinds of OD layers, with three OD layers per repeat unit (Fig. 1):

L_{3n} — OD layer (denoted Oc in the following) containing the plane of octahedrally coordinated cations plus halves of the adjacent planes of apical O atoms and of OH groups at the same level; symmetry $P(\bar{3})12/m$ (pyrophyllite), $H(\bar{3})12/m$ (talc), origin at a void (pyrophyllite), or at any octahedral position (talc).

$L_{3n \pm 1}$ — OD layer (denoted Tet in the following) containing basal O atoms, tetrahedral cations and halves of the apical O atoms and of the OH groups at the same level — all belonging to a tetrahedral silicate sheet; symmetry $P(6)mm$, origin at the hexad.

From the structural investigations [11]—[19] it follows that the origin of any OD layer L_n can be displaced relative to that of L_{n-1} in the $X_1 X_2$ projection, only by one of the six vectors denoted in Fig. 2 by characters 0 to 5, and that the pairs of adjacent OD layers $(L_{3n-1}; L_{3n})$, $(L_{3n}; L_{3n+1})$ and $(L_{3n+1}; L_{3n+2})$ remain geometrically equivalent in any structure within the pyrophyllite or talc family, respectively, independently of the actual stacking mode. Moreover, the translation groups of the two kinds of OD layers are either identical (pyrophyllite) or one of them is a subgroup of the other (talc). These facts prove the OD character of the investigated structures. The sequence of OD layers and their polarity are typical for category I, the symbols of the OD groupoid family [20] for the two investigated mineral families read:

pyrophyllite

$$P(\bar{3})12/m \qquad P(6)mm$$

$$\left[-\frac{1}{3}, -\frac{1}{3}\right] \qquad \left\{2_{-\frac{1}{3}} \, 2_{\frac{2}{3}} \, 2_{-\frac{1}{3}} \begin{pmatrix} \bar{3} \\ \bar{6} \\ n_0 \frac{2}{3} \end{pmatrix} 2_{\frac{1}{3}} \, 2 \, 2_{-\frac{1}{3}} \right\}, \tag{1}$$

talc

$$H(\bar{3})12/m \qquad P(6)mm$$

$$\left[-\frac{1}{3}, -\frac{1}{3}\right] \qquad \left\{2_{-\frac{1}{3}} \, 2_{\frac{2}{3}} \, 2_{-\frac{1}{3}} \begin{pmatrix} \bar{3} \\ \bar{6} \\ n_0 \frac{2}{3} \end{pmatrix} 2_{\frac{1}{3}} \, 2 \, 2_{-\frac{1}{3}} \right\}.$$

In the first line there are the layer groups of the two kinds of OD layers starting with Oc, in the second line between them — the components of the displacement vector $\bar{\mathbf{v}}_{3n, 3n+1}$ separating the origins of L_{3n} and L_{3n+1} in the $X_1 X_2$ projection. Any two adjacent tetrahedral OD layers L_{3n+1} and L_{3n+2} are geometrically equivalent with opposite sense of their polarity. The ϱ-operations [20] converting L_{3n+1} into L_{3n+2} are indicated in the second line in braces; the seven places of this expression refer to the directions X_1, X_2, $X_3(Z)$ Y_1, Y_2, Y_3, respectively (Fig. 3) [1], [21]. It should be noted here that either of the expressions in the second line refers to only one of all possible positions of Tet relative to Oc (square

2

PACKETS	STRUCTURAL SCHEME	OD LAYERS		POLARITY OF OD LAYERS
P_3		L_4		
		L_3		
P_2		L_2		
P_1		L_1	Tet	polar
		L_0	Oc	nonpolar
P_0		L_{-1}	Tet	polar

Fig. 1. Schematic representation of pyrophyllite or talc structures, showing OD layers, OD packets, their labelling, and indicating the polarity of OD layers.
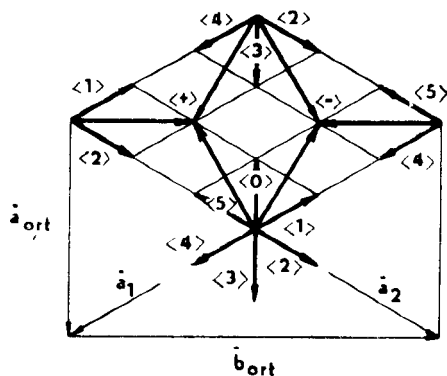

Fig. 2. Displacement vectors ⟨v⟩, their relation to the basic vectors $\bar{a}_1$, $\bar{a}_2$ and their conventional characters:

$$⟨0⟩ = (-1/3, -1/3); \quad ⟨1⟩ = (-1/3, 0); \quad ⟨2⟩ = (0, 1/3);$$
$$⟨3⟩ = (1/3, 1/3); \quad ⟨4⟩ = (1/3, 0); \quad ⟨5⟩ = (0, -1/3);$$
$$⟨*⟩ = (0, 0); \quad ⟨+⟩ = (-1/3, 1/3); \quad ⟨-⟩ = (1/3, -1/3).$$

brackets) and *Tet* relative to the preceding *Tet* (braces), respectively; any of the remaining possible positions could be used equally well [20] (see also Appendix).

The number of all possible, geometrically equivalent positions $Z_{p(p-1)}$ of the OD layer L_p relative to L_{p-1} follows from the symmetry of individual OD layers and from any one of their possible relative positions as indicated in the symbol (1). The resulting NFZ relations [1] (N_p is the order of the layer group of L_p, F is the order of the layer group of the pair $(L_p; L_{p+1})$) are summarized in Table I. They are closely related to those for dioctahedral (pyrophyllite) and triocta-hedral (talc) micas, respectively.
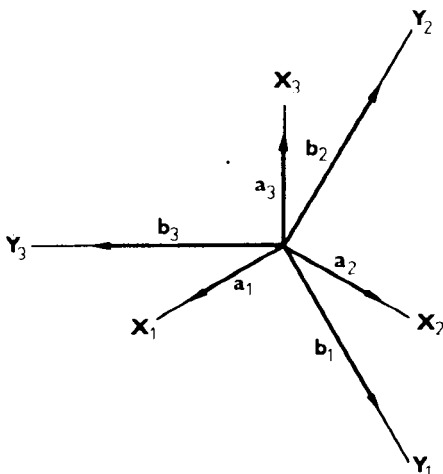
Fig. 3. Axial system used in this paper. $1\,\bar{b}_i\,1 = 1\,\bar{a}_i\,1\,\sqrt{3}$.

Table I

The NFZ relations for the pyrophyllite and talc family with hexagonal symmetry of tetrahedral OD layers

OD layer L_p		layer group	N_p	F	$Z_{p(p-1)}$
		Pyrophyllite family			
L_{3n-1}	(Tet)	$P(6)mm$	12		
				2	
L_{3n}	(Oc)	$P(\bar{3})12/m$	6	2	6
L_{3n+1}	(Tet)	$P(6)mm$	12	2	3
L_{3n+2}	(Tet)	$P(6)mm$	12		6
		Talc family			
L_{3n-1}	(Tet)	$P(6)mm$	12	6	
L_{3n}	(Oc)	$H(\bar{3})12/m$	18	6	2
L_{3n+1}	(Tet)	$P(6)mm$	12	2	3
L_{3n+2}	(Tet	$P(6)mm$	12		6

OD PACKETS, POLYTYPE SYMBOLS AND PICTORIAL REPRESENTATION OF POLYTYPES

According to the definition of OD packets [22], any pyrophyllite or talc packet corresponds to one half of the 2 : 1 layer. Therefore it consists of one half of *Oc* and of the entire adjacent *Tet;* even- and odd-numbered packets are geometrically equivalent. They differ only in the sense of their polarity and alternate regularly in the structure (Fig. 1). Any pyrophyllite packet has the symmetry *Cm* and

can appear in only six different orientations depending on the position of the origin of *Oc* relative to that of *Tet*. The situation is completely analogous to that in dioctahedral micas [7]. Thus we shall denote these orientations by numbers 0 to 5 with a dot (.) to their right (even-numbered packets) or to their left (odd-numbered packets) and represent them by an appropriately oriented isosceles triangle (empty and full for even-numbered and odd-numbered packets, respectively), with a rod attached to its base. The apex of any such triangle marks the origin of the packet and coincides with the origin of the corresponding *Tet*, the end of the rod marks the position of the origin of *Oc*. An even- and an odd-numbered packet with the same orientational characters are represented by inversion-related triangles [7]. The sequence of packets in any pyrophyllite polytype can be characterized by a fully descriptive polytype symbol:

$$T_0 \cdot T_1 \quad T_2 \cdot T_3 \quad T_4 \cdot T_5 \ldots$$
$$\quad v_{01} \quad v_{12} \quad v_{23} \quad v_{34} \quad v_{45}$$

$$(2)$$

where T_i are orientational characters (numbers 0 to 5) of individual packets and $v_{i,i+1}$ are the displacement characters (numbers 0 to 5) referring to the relative shifts of their origins. The meaning of the characters is shown in Fig. 2. Such a sequence can also be represented by a numbered sequence of isosceles triangles with rods as shown in Fig. 4a (right). Evidently, the symbol has the same appea-
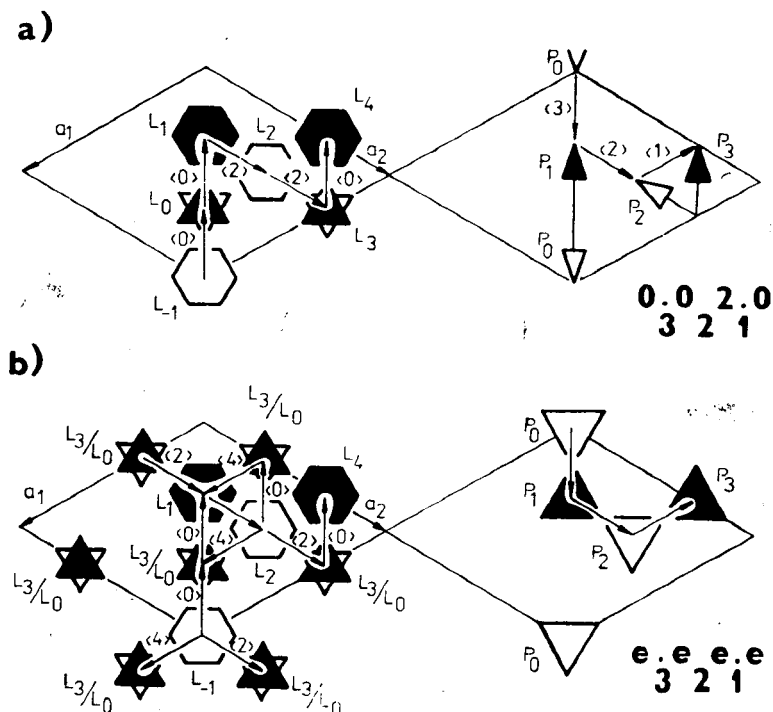

Fig. 4. Sequence of five OD layers (left) and the corresponding sequence of four OD packets (right) in a pyrophyllite (a) and in a talc (b) structure. The OD layers and OD packets are numbered according to their sequence, L_m/L_n means a coincidence of these layers in the X_1, X_2 projection. Displacement vectors $\langle v \rangle$ are also indicated (cf. Fig. 2) when necessary.

rance as that for micas [7] with the difference that the displacement characters $v_{2n+1, 2n+2}$ cannot be * (for a zero vector) since there is no anchoring effect between L_{3n+1} and L_{3n+2} here.

A similar reasoning holds for talc polytypes. The difference is only that the symmetry of their packets is $P(3)1m$ and that they can appear in only two orientations denoted — as in trioctahedral micas — e and u. Any of them will be represented by an equilateral triangle whose centre marks its origin (coinciding with that of Tet) and whose sides point to the three translationally equivalent origins of Oc. The symbol of any talc polytype and its pictorial representation is similar as in pyrophyllite (Fig. 4b).

Fig. 4 shows a part of a pyrophyllite polytype (a) and a part of a talc polytype (b) represented in the left part of the figure as a sequence of five OD layers, in the right part as the corresponding sequence of four OD packets. The geometrical figures chosen for the OD layers not only possess the relevant symmetries but they also carry useful crystallochemical information: the hexagons representing Tet have the same orientations as those drawn through the tetrahedrally coordinated Si atoms or apical O atoms, and their centres coincide in projection with the OH groups whose halves belong also to the adjacent Oc. The orientations of the empty and full equilateral triangles of the triangular stars representing Oc are the same as the orientations of the lower and upper bases of coordination octahedra in the octahedral sheet — their centres coincide with the origins of Oc. Since the translation group of Oc in pyrophyllite is P, there is only one such triangular star per unit mesh and one displacement vector suffices to express the orientation of the packets, e.g. $\langle 0 \rangle$ for P_0, P_1 and P_3. The displacement vector $\overline{\mathbf{v}}_{01} = \langle 3 \rangle$ is the vector sum of two vectors $\langle 0 \rangle$ (Fig. 2). The symbol of the sequence discussed is given in the right part of Fig. 4a. The translation group of Oc in talc is triply primitive (H) and its three origins per unit mesh P can be reached from the origin of Tet simultaneously by three vectors — in Fig. 4b by those with even characters, i.e. $\langle 0 \rangle \wedge \langle 2 \rangle \wedge \langle 4 \rangle$, and the same holds for the position of Tet relative to the preceding Oc. The orientational characters of all packets in Fig. 4b are thus denoted by e.

The position of L_{3n+2} relative to L_{3n+1} as well as that of L_{3n+1} relative to L_{3n} indicated in the symbol of the OD groupoid family (1) is the same as shown in Fig. 4.

The characters T_{2n}, T_{2n+1} and $v_{2n, 2n+1}$ describing one pair of adjacent packets (P_{2n}; P_{2n+1}) are not mutually independent. Due to the octahedral coordination of cations or voids within the octahedral sheet, the orientational characters T_{2n} and T_{2n+1} must be of the same parity, whereas $v_{2n, 2n+1}$ corresponding to their vector sum is of the opposite parity (cf. Fig. 2). Only $v_{2n+1, 2n+2}$ is independent if idealized hexagonal symmetry of tetrahedral OD layers is considered. This is why the symbol of pyrophyllite polytypes in its full form (2) is redundant (i.e. the characters $v_{2n, 2n+1}$ in it are redundant) and for some purposes also its abbreviated form can be used. E.g. the packet sequence shown in Fig. 4a can be described as $\frac{0.0\ 2.0}{2}$ or simply $00_2 20$ because the characters $v_{2n+1, 2n+2}$ mark unambiguously the interlayer region. The situation is inverted in the talc family, where orientational characters are redundant since T_{2n} and T_{2n+1} must both be e if $v_{2n, 2n+1}$ is odd and vice versa. An abbreviated symbol in this case would consist simply of a string of displacement characters in which however $v_{2n, 2n+1}$

has to be distinguished — e.g. by a dot over it — from $v_{2n+1,2n+2}$. For the packet sequence in Fig. 4b we obtain then $32\dot{1}$.

The symbolism used in this paper is very similar to that introduced by Zvyagin [18] who uses the form $s_i s_j t_k s_l s_m t_n \ldots$ or simply $ij_k lm_n \ldots$, where $i = 6 - T_{2n}$, $j = 6 - T_{2n+1}$, $k = 6 - v_{2n+1,2n+2}$, etc., so that the sequence shown in Fig. 4a (pyrophyllite) reads $s_6 s_6 t_4 s_4 s_6$ or $66_4 46$. For talc polytypes he selects the path $s_i s_l$ (one of three possible paths from the origin of L_{3n-1} through the three origins of L_{3n} to the origin of L_{3n+1}) which passes through the inversion centre of the 2 : 1 layer, as representative for his symbols, and thus for the sequence shown in Fig. 4b he obtains $s_6 s_6 t_4 s_2 s_2$ or $66_4 22$. The Zvyagin symbols thus do not indicate whether they refer to a talc polytype or to a pyrophyllite polytype with centrosymmetric 2 : 1 layers, and this information has to be given in addition.

SYMBOLS AND SYMMETRY OF POLYTYPES

Since the fully descriptive symbols characterize completely the structure of any polytype, they reflect also both total and partial symmetry of any sequence of OD packets. It is necessary to find out only what influence have the coincidence operations relevant to the investigated family on the orientational and displacement characters and to compile a table of the corresponding conversions. From the very character of our symbolism it follows that only point operations isogonal to those which can be encountered in the investigated family, need be listed. Table II gives the conversions of characters corresponding to coincidence operations transforming packet P_p into P_q: for τ-operations $q - p = 2n$, for ϱ-operations $q - p = 2n + 1$. We shall illustrate the application of this table by means of some examples.

Any pyrophyllite packet has the symmetry Cm, the order of the point group m isogonal to it is $N = 2$ and therefore there are always two operations converting it into another packet: one congruent, the other enantiomorphous. Any two adjacent packets can be related by ϱ-operations only. Let us take the pair $(P_0; P_1)$ with the symbol $\begin{smallmatrix} 2.2 \\ 5 \end{smallmatrix}$ (Fig. 5a). With the help of Table II it can be found that P_0 is converted into P_1 by a two-fold rotation about an axis parallel to Y_2 (Fig. 3), i.e. $[\ldots (.) . 2 .]$ as well as by an inversion. Since the same statement holds also for the conversion of P_1 into P_0 and then also for v_{01} it follows that both these operations have a reverse continuation which means that these operations are total, i.e. they are symmetry operations for the packet pair $\begin{smallmatrix} 2.2 \\ 5 \end{smallmatrix}$. This fact can be expressed in the "OD language": $_{01}\varrho \leftrightarrow {}_{10}\varrho$ and the operation with such a reverse continuation is denoted by the superscript $+$, e.g. $[I]^+$. In the packet pair $\begin{smallmatrix} 0.2 \\ 1 \end{smallmatrix}$ (Fig. 5c) P_0 is converted into P_1 by a two-fold rotation $[\ldots (.) 2 ..]^+$ (i.e. with reverse continuation) and by a three-fold rotoinversion $[(\bar{3})^{-1}]^-$ (without reverse continuation). Only $[\ldots (.) 2 ..]^+$ converts also v_{01} into itself (Table II) and therefore only this coincidence operation becomes a symmetry operation for the packet pair. The pairs $\begin{smallmatrix} .2\ 2. \\ 1 \end{smallmatrix}$ (Fig. 5b) and $\begin{smallmatrix} .3\ 1. \\ 3 \end{smallmatrix}$ (Fig. 5d) can be treated in the same way. It should only be realized that the operation $[\ldots (.) . 2 .]^-$ here corresponds in fact to a two-fold screw operation.
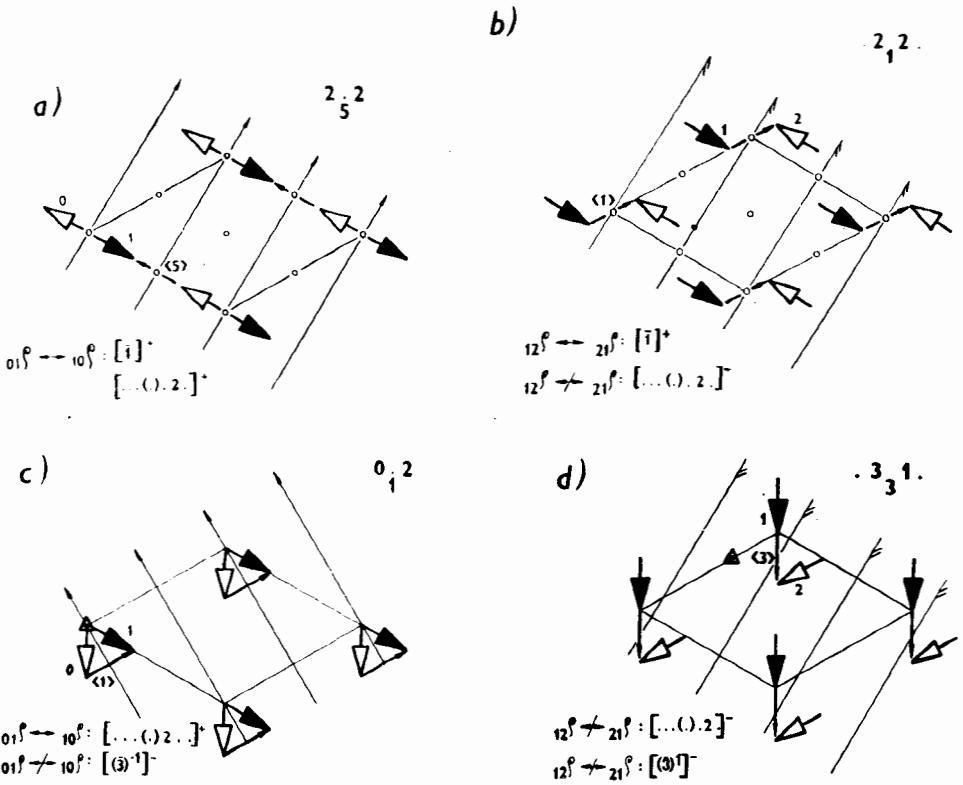
Fig. 5. Four typical pairs of adjacent pyrophyllite packets $(P_0; P_1)$ (a, c) and $(P_1; P_2)$ (b, d), together with their respective symbols. Indicated are also ϱ — coincidence operations as well as the character of these (presence or absence of a reverse continuation). The packets are numbered according to their sequence.

Table II

Conversions of characters

τ point operation	Character								ϱ point operation
	0	1	2	3	4	5	e	u	
1	0	1	2	3	4	5	e	u	$\bar{1}$
$(6)^{-1}$	1	2	3	4	5	0	u	e	$(\bar{6})^{-1}$
$(3)^{-1}$	2	3	4	5	0	1	e	u	$(\bar{3})^{-1}$
$(2)^1$	3	4	5	0	1	2	u	e	$\bar{2}$ or $m \perp Z$
$(3)^1$	4	5	0	1	2	3	e	u	$(\bar{3})^1$
$(6)^1$	5	0	1	2	3	4	u	e	$(\bar{6})^1$
$m..(.)...$	5	4	3	2	1	0	u	e	$2..(.)...$
$...(.).m.$	4	3	2	1	0	5	e	u	$...(.).2.$
$..m(.)...$	3	2	1	0	5	4	u	e	$..2(.)...$
$...(.)m..$	2	1	0	5	4	3	e	u	$...(.)2..$
$.m.(.)...$	1	0	5	4	3	2	u	e	$.2.(.)...$
$...(.)..m$	0	5	4	3	2	1	e	u	$...(.)..2$

8

It can be shown that the only ϱ-operations which can have a reverse continuation in the pyrophyllite and talc family are two-fold rotations, an inversion and a reflection in a plane perpendicular to Z.

In the packet triple $\begin{smallmatrix} 2.2\ 2. \\ 5\ 1 \end{smallmatrix}$ (combination of Fig. 5a and 5b) P_0 is converted into P_2 by two τ-operations which can be identified with the help of Table II as a glide operation in a plane perpendicular to Y_2, i.e. $[\ldots(.).m.]$ and a translation. The circumstance whether a $_{n,\,n+1}\varrho$-operation has a reverse continuation or not is of a fundamental importance for the derivation of MDO polytypes (see below).

Any talc packet has the symmetry $P(3)1m$, the order of the point group $31m$ isogonal to it is $N = 6$ and therefore there are always six coincidence operations converting it into another packet, three of them congruent, the other three enantiomorphous. These operations can also be found with the help of Table II.

In an analogous way the symmetry of any sequence of packets can be determined from its symbol. It should only be kept in mind that:

a) A $_{n,\,n+1}\varrho^{(i)}$ coincidence operation becomes a symmetry operation for a sequence of packets if and only if it converts this sequence into itself, i.e. if it converts any P_{n-p} into P_{n+p+1} and vice versa, so that

$$_{n-p,\,n+p+1}\varrho^{(i)} \leftrightarrow {}_{n+p+1,\,n-p}\varrho^{(i)}. \tag{3}$$

As a consequence, the point operation isogonal to $\varrho^{(i)}$ converts any orientational character T_{n-p} into T_{n+p+1} and any displacement character $v_{n-p,\,n-p+1}$ into $v_{n+p,\,n+p+1}$ and vice versa, for any integer n and any positive integer p.

b) A $_{n,\,n+k}\tau^{(i)}$ coincidence operation (k — an even integer) becomes a symmetry operation for a sequence of packets if and only if it converts any P_{n+p} into P_{n+p+k} so that

$$_{n,\,n+k}\tau^{(i)} \leftrightarrow {}_{n+p,\,n+p+k}\tau^{(i)}. \tag{4}$$

As a consequence, the point operation isogonal to $\tau^{(i)}$ converts any orientational character T_{n+p} into T_{n+p+k} and any displacement character $v_{n,\,n+1}$ into $v_{n+p+k,\,n+p+k+1}$ for any integer n and p.

Let us take as an example the periodic four-packet polytype with the symbol $\begin{vmatrix} 5.5 & 1.1 \\ 2 & 0 & 4 & 0 \end{vmatrix}$ and analyze e.g. the sequence

$$\ldots 5.5 \quad 1.1 \quad 5.5 \quad 1.1 \ldots$$
$$2 \quad 0 \quad 4 \quad 0 \quad 2 \quad 0 \quad 4$$
$$(\ldots P_0\,P_1\,P_2\,P_3\,P_4\,P_5\,P_6\,P_7\ldots P_n\ldots)$$

With the help of Table II it can be found that e.g. the $_{45}[\bar{1}]$ is a total symmetry operation for this polytype since the relation (3) holds for any $p > 0$, whereas the $_{45}[\ldots(.).2.]$ is only partial since (3) holds only for $p \equiv 0$ (*mod 4*). On the other hand e.g. the $_{12}[\ldots(.)..2]$ turns out to be total, whereas the corresponding enantiomorphous coincidence operation $_{12}[(\bar{3})^{-1}]$ converts only P_1 into P_2, it has no reverse continuation and it is thus neither a partial symmetry operation for the pair $(P_1;\,P_2)$ nor a symmetry operation for the whole polytype.

A systematic analysis of this sequence reveals the presence and character of the following operations:

a) $_{4m,4m+1}[I]^+$, $_{4m+1,4m+2}[\ldots(.)..2]^+$,

$_{4m+2,4m+3}[I]^+$, $_{4m+3,4m+4}[\ldots(.)..2]^+$ (m — any integer)

— total symmetry operations, (3) holds for any p,

b) $_{4m,4m+1}[\ldots(.).2.]^+$ and $_{4m+2,4m+3}[\ldots(.)2..]^+$

— partial symmetry operations, (3) holds only for $p \equiv 0 \ (mod\ 4)$,

c) $_{4m+1,4m+2}[(\bar{3})^{-1}]^-$ and $_{4m+3,4m+4}[(\bar{3})]^-$

— coincidence operations, (3) does not hold at all.

The only non-trivial τ-operation is the glide operation isogonal to $[\ldots(.)..m]$ since the relation (4) holds for any n, p integer and for $k = 2$ (and thus also for $k = 6, 10, 14, \ldots$). Keeping in mind the symmetry of individual packets it follows that the space group of the investigated polytype is $C12/c1$.

MDO POLYTYPES

All MDO polytypes of pyrophyllite can be derived according to the standard procedures ([23], [24], see also [8]), forming first all those packet triples $(P_0; P_1; P_2)$ compatible with the family, for which there exists at least one $_{01}[\varrho^{(t)}]^+$ and at least one $_{12}[\varrho^{(j)}]^+$ operation. There are three non-congruent packet pairs $(P_0; P_1)$, i.e. $\dfrac{0.0\ 0.2}{3}$, $\dfrac{0.2}{1}$ and $\dfrac{0.4}{5}$ (if the first packet is taken in the standard orientation $T_0 = 0$): the first pair is related by $[I]^+$ as well as by $[\ldots(.)..2]^+$ (see Table II), the second only by $[\ldots(.)2..]^+$, the third only by $[\ldots(.).2.]^+$. As far as $(P_1; P_2)$ is concerned, there are 36 non-congruent such pairs, but in a similar way it can be shown that only $\dfrac{.00.}{0}$, $\dfrac{.00.}{3}$, $\dfrac{.00.}{1}$, $\dfrac{.00.}{5}$, $\dfrac{.00.}{2}$, $\dfrac{.00.}{4}$, $\dfrac{.02.}{1}$, $\dfrac{.04.}{5}$, $\dfrac{.04.}{2}$ and $\dfrac{.02.}{4}$ need to be considered — the others possess no ϱ-operation with a reverse continuation. In the next step, for any combination of permitted pairs $(P_0; P_1)$ with $(P_1; P_2)$, all $_{02}\tau$-operations as products $_{01}[\varrho^{(t)}]^+ \cdot _{12}[\varrho^{(j)}]^+$ have to be found and used as generating τ-operations with a continuation in the entire polytype considered. The periodic polytype derived in this way will contain only two kinds of triples of consecutive OD layers $(L_0; L_1; L_2)$ and $(L_1; L_2; L_3)$ and this is evidently the absolute minimum of kinds in the pyrophyllite family. Any combination of $(P_0; P_1)$ for which there exists always at least one $_{01}[\varrho^{(t)}]^+$ with $(P_1; P_2)$ for which there exists no $_{12}[\varrho^{(j)}]^+$ would result in a polytype containing three kinds of triples of consecutive OD layers (cf. Fig. 5) and violating thus the stipulation for MDO structures [23], [24].

As an example for the derivation of MDO polytypes we may take the pair $\dfrac{0.2}{1}$ related by $_{01}[\ldots(.)2..]^+$ and combine it with the pair $\dfrac{.00.}{3}$ related in the appropriate orientation $\dfrac{.22.}{5}$ by $_{12}[I]^+$ as well as by $_{12}[\ldots(.).2.]^+$. For the packet triple $\dfrac{0.2\ 2.}{1\ 5}$ thus formed we obtain two $_{02}\tau$-operations which lead to two MDO polytypes:

$$_{02}\tau^{(1)} = _{01}[\ldots(.)2..]^+ \cdot _{12}[I]^+ = _{02}[\ldots(.)m..] \text{ and}$$

$$_{02}\tau^{(2)} = _{01}[\ldots(.)2..]^+ \cdot _{12}[\ldots(.).2.]^+ = _{02}[(3)^{-1}]$$

Table III

MDO polytypes of pyrophyllite and talc. Enantiomorphous pairs (if any) are listed under the same number

Pyrophyllite, subfamily A

No.	Polytype symbol		basic vectors	space group
1	$\begin{vmatrix} 0.0 \\ 3\ 3 \end{vmatrix}$		$\bar{a},\ \bar{b},\ \bar{c}_0 - \bar{a}/3$	$C12/m1$
2	$\begin{vmatrix} 2.4 \\ 3\ 3 \end{vmatrix}$			$C121$
		$\begin{vmatrix} 4.2 \\ 3\ 3 \end{vmatrix}$		
3	$\begin{vmatrix} 2.2 \\ 5\ 1 \end{vmatrix}$	[16], [18], [19], Fig. 6a		$C\bar{1}$
4	$\begin{vmatrix} 3.3\ 3.3 \\ 0\ 4\ 0\ 2 \end{vmatrix}$	[18]	$\bar{a},\ \bar{b},\ 2\bar{c}_0 - \bar{a}/3$	$C12/c1$
5	$\begin{vmatrix} 1.5\ 5.1 \\ 0\ 4\ 0\ 2 \end{vmatrix}$			
6	$\begin{vmatrix} 5.1\ 1.5 \\ 0\ 4\ 0\ 2 \end{vmatrix}$			
7	$\begin{vmatrix} 5.5\ 1.1 \\ 2\ 0\ 4\ 0 \end{vmatrix}$	[11], [18]		
8	$\begin{vmatrix} 5.1\ 1.5 \\ 0\ 0\ 0\ 0 \end{vmatrix}$			
9	$\begin{vmatrix} 0.0\ 2.2\ 4.4 \\ 3\ 1\ 5\ 3\ 1\ 5 \end{vmatrix}$		$\bar{a}_1,\ \bar{a}_2,\ 3\bar{c}_0$	$P3_2 12$
		$\begin{vmatrix} 0.0\ 4.4\ 2.2 \\ 3\ 5\ 1\ 3\ 5\ 1 \end{vmatrix}$		$(P3_1 12)$
10	$\begin{vmatrix} 2.4\ 4.0\ 0.2 \\ 3\ 1\ 5\ 3\ 1\ 5 \end{vmatrix}$			
		$\begin{vmatrix} 4.2\ 2.0\ 0.4 \\ 3\ 5\ 1\ 3\ 5\ 1 \end{vmatrix}$		
11	$\begin{vmatrix} 4.2\ 0.4\ 2.0 \\ 3\ 1\ 5\ 3\ 1\ 5 \end{vmatrix}$			
		$\begin{vmatrix} 2.4\ 0.2\ 4.0 \\ 3\ 5\ 1\ 3\ 5\ 1 \end{vmatrix}$		

Talc, subfamily A

No.	Polytype symbol		basic vectors	space group
1	$\begin{vmatrix} e.e \\ 3\ 3 \end{vmatrix}$		$\bar{a},\ \bar{b},\ \bar{c}_0 - \bar{a}/3$	$C12/m1$
2	$\begin{vmatrix} e.e \\ 5\ 1 \end{vmatrix}$	[17. [18], Fig. 6b		$C\bar{1}$
3	$\begin{vmatrix} u.u\ u.u \\ 0\ 4\ 0\ 2 \end{vmatrix}$	[18]	$\bar{a},\ \bar{b},\ 2\bar{c}_0 - \bar{a}/3$	$C12/c1$
4	$\begin{vmatrix} u.u\ u.u \\ 2\ 0\ 4\ 0 \end{vmatrix}$			
5	$\begin{vmatrix} e.e\ e.e\ e.e \\ 3\ 1\ 5\ 3\ 1\ 5 \end{vmatrix}$		$\bar{a}_1,\ \bar{a}_2,\ 3\bar{c}_0$	$P3_2 12$
		$\begin{vmatrix} e.e\ e.e\ e.e \\ 3\ 5\ 1\ 3\ 5\ 1 \end{vmatrix}$		$(P3_1 12)$

Table III (continued)

Pyrophyllite, subfamily B

No.	Polytype symbol	basic vectors	space group
12	$\begin{vmatrix} 0.0 \\ 3\ 0 \end{vmatrix}$	$\bar{a}, \bar{b}, \bar{c}_0$	$C12/n1$
13	$\begin{vmatrix} 2.4 \\ 3\ 0 \end{vmatrix}$		$C121$
	$\begin{vmatrix} 4.2 \\ 3\ 0 \end{vmatrix}$		
14	$\begin{vmatrix} 2.2 \\ 5\ 4 \end{vmatrix}$	$\bar{a}, \bar{b}, \bar{c}_0 - \bar{b}/3$	$C\bar{1}$
15	$\begin{vmatrix} 3.\ 33.\ 3 \\ 0\ 1\ 0\ 5 \end{vmatrix}$	$\bar{a}, \bar{b}, 2\bar{c}_0$	$C12/c1$
16	$\begin{vmatrix} 1.5\ 5.1 \\ 0\ 1\ 0\ 5 \end{vmatrix}$		
17	$\begin{vmatrix} 5.1\ 1.5 \\ 0\ 1\ 0\ 5 \end{vmatrix}$		
18	$\begin{vmatrix} 5.5\ 1.1 \\ 2\ 3\ 4\ 3 \end{vmatrix}$		
19	$\begin{vmatrix} 5.\ 11.5 \\ 0\ 3\ 0\ 3 \end{vmatrix}$		
20	$\begin{vmatrix} 0.0\ 2.2\ 4.4 \\ 3\ 4\ 5\ 0\ 1\ 2 \end{vmatrix}$	$\tilde{a}_1, \tilde{a}_2, 3\bar{c}_0$	$P3_212$
	$\begin{vmatrix} 0.0\ 4.4\ 2.2 \\ 3\ 2\ 1\ 0\ 5\ 4 \end{vmatrix}$		$(P3_112)$
21	$\begin{vmatrix} 2.4\ 4.0\ 0.2 \\ 3\ 4\ 5\ 0\ 1\ 2 \end{vmatrix}$		
	$\begin{vmatrix} 4.2\ 2.0\ 0.4 \\ 3\ 2\ 1\ 0\ 5\ 4 \end{vmatrix}$		
22	$\begin{vmatrix} 4.2\ 0.4\ 2.0 \\ 3\ 4\ 5\ 0\ 1\ 2 \end{vmatrix}$		
	$\begin{vmatrix} 2.4\ 0.2\ 4.0 \\ 3\ 2\ 1\ 0\ 5\ 4 \end{vmatrix}$		

Talc, subfamily B

No.	Polytype symbol	basic vectors	space group
6	$\begin{vmatrix} e.e \\ 3\ 0 \end{vmatrix}$	$\bar{a}, \bar{b}, \bar{c}_0$	$C12/m1$
7	$\begin{vmatrix} e.e \\ 5\ 4 \end{vmatrix}$	$\bar{a}, \bar{b}, \bar{c}_0 - \bar{b}/3$	$C\bar{1}$
8	$\begin{vmatrix} u.u\ u.u \\ 0\ 1\ 0\ 5 \end{vmatrix}$	$\bar{a}, \bar{b}, 2\bar{c}_0$	$C12/c1$
9	$\begin{vmatrix} u.u\ u.u \\ 2\ 3\ 4\ 3 \end{vmatrix}$		
10	$\begin{vmatrix} e.e\ e.e\ e.e \\ 3\ 4\ 5\ 0\ 1\ 2 \end{vmatrix}$	$\bar{a}_1, \bar{a}_2, 3\bar{c}_0$	$P3_212$
	$\begin{vmatrix} e.e\ e.e\ e.e \\ 3\ 2\ 1\ 0\ 5\ 4 \end{vmatrix}$		$(P3_112)$

the first leading to the polytype $\begin{vmatrix} 0.2 & 2.0 \\ 1 & 5 & 1 & 3 \end{vmatrix}$, the second to the polytype $\begin{vmatrix} 0.2 & 2.4 & 4.0 \\ 1 & 5 & 3 & 1 & 5 & 3 \end{vmatrix}$. The first polytype has to be re-oriented by an anticlockwise rotation about the Z axis in order to bring it into the conventional standard orientation $\begin{vmatrix} 5.1 & 1.5 \\ 0 & 4 & 0 & 2 \end{vmatrix}$. It has the space group $C12/c1$ and basic vectors $\bar{\boldsymbol{a}}$, $\bar{\boldsymbol{b}}$, $2\bar{\boldsymbol{c}}_0 - \bar{\boldsymbol{a}}/3$, where $\bar{\boldsymbol{c}}_0 \| Z$ and $|\bar{\boldsymbol{c}}_0|$ corresponds to the "width" of any packet pair. The second polytype has the space group $P3_12$, basic vectors $\bar{\boldsymbol{a}}_1$, $\bar{\boldsymbol{a}}_2$, $3\bar{\boldsymbol{c}}_0$ and we prefer to write it so that $v_{01} = 3$, thus $\begin{vmatrix} 2.4 & 4.\bullet & 0.2 \\ 3 & 1 & 5 & 3 & 1 & 5 \end{vmatrix}$.

In this way all MDO polytypes for the pyrophyllite family have been derived. The MDO polytypes in the talc family could be obtained in a similar way, but it was easier to increase simply the symmetry of packets by substituting e and u for all even and odd orientational characters, respectively and exclude polytypes which have been obtained more than once. The results are summarized in Table
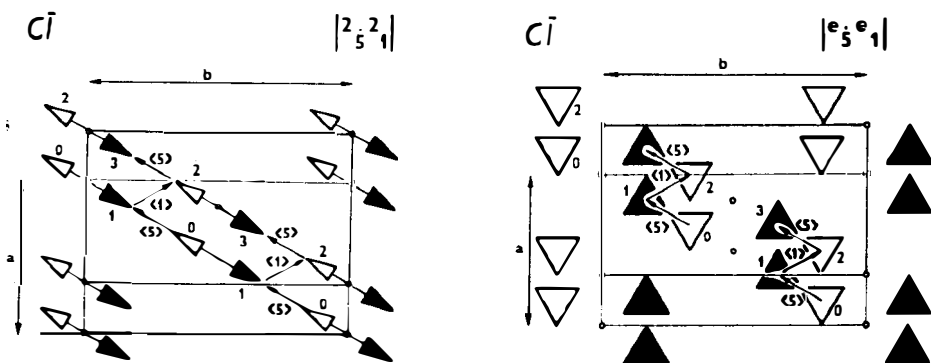

Fig. 6. Pictorial representation of a pyrophyllite (a) and a talc (b) polytype. The packets are numbered according to their sequence; displacement vectors, polytype symbols and space groups are also given.

III; all MDO polytypes are subdivided into two subfamilies: with $v_{2n+1, 2n+2}$ of the same, and of the opposite parity as T_n, respectively. All in all there are 2×15 non-congruent (2×11 non-equivalent) MDO polytypes in the pyrophyllite family and 2×6 (2×5) MDO polytypes in the talc family. According to Zvyagin [18] only the polytypes belonging to the subfamilies with $v_{2n+1, 2n+2}$ of the opposite parity as T_n have been observed so far (see also below). A pictorial representation of two commonnest polytypes of pyrophyllite and talc is in Fig. 6.

Out of the six non-equivalent one- and two-layer (two- and four- packet) pyrophyllite structures with centrosymmetric 2:1 layers with the symbols $66_366\ldots$, $22_122\ldots$, $33_233_433\ldots$, $11_655_611\ldots$, $55_211_455\ldots$, and $11_433_411\ldots$ derived by Zvyagin [18], the first four are MDO polytypes identical with our polytypes No 1, 3, 4 and 7, respectively (Table III). The remaining two are not MDO polytypes since, as evident from their converted symbols $\begin{vmatrix} 5.5 & 1.1 \\ 2 & 2 & 4 & 4 \end{vmatrix}$ and $\begin{vmatrix} 1.1 & 3.3 \\ 4 & 4 & 0 & 4 \end{vmatrix}$, they contain packet pairs $(P_1; P_2)$ for which there is no $_{12}[\varrho^{(i)}]^+$.

EFFECT OF DITRIGONALIZATION

Tetrahedral sheets in sheet silicates are always more or less ditrigonalized in order to match up with adjacent octahedral sheets. We shall now investigate the effect of such a ditrigonalization on the OD interpretation of pyrophyllite and talc structures, considering the structural models with "ideal ditrigonalization" [25] in which the symmetry of any Tet will be lowered from $P(6)mm$ to $P(3)1m$, leaving the symmetry of any Oc unchanged.

The ditrigonalization of Tet in the structures of both pyrophyllite $\begin{vmatrix} 2.1 \\ 5 \quad 1 \end{vmatrix}$ [19]

and talc $\begin{vmatrix} e.e \\ 5 \quad 1 \end{vmatrix}$ [17] with space groups $C\bar{1}$ is of the type "positive-positive" [26]. Taking these structures as representatives for their respective families, we obtain the following symbols of the corresponding OD groupoid families: pyrophyllite

$$P(\bar{3})12/m \qquad P(3)1m$$

$$\left[0, \frac{1}{3}\right] \qquad \left\{ 1 \; 1 \; 1 \begin{pmatrix} 3 \\ \bar{6} \end{pmatrix} 2 \; 2_{\frac{1}{3}} \; 2_{-\frac{1}{3}} \right\},$$

talc $\qquad H(\bar{3})12/m \qquad P(3)1m$ $\hspace{5cm}$ (5)

$$\left[0, \frac{1}{3}\right] \qquad \left\{ 1 \; 1 \; 1 \begin{pmatrix} \bar{1} \\ 3 \\ \bar{6} \end{pmatrix} 2 \; 2_{\frac{1}{3}} \; 2_{-\frac{1}{3}} \right\}.$$

The NFZ relations following from this kind of stacking are in Table IV. The fact that the expression in square brackets and that in braces of (5) for pyrophyllites correspond to the displacement vectors with characters 2 and 1, respectively, that $Z_{3n+1(3n)} = 3$, and that $Z_{3n+2(3n+1)} = 3$ implies that the ditrigonalization permits only polytypes in whose symbols *all orientational characters are of the same parity, which is opposite to the parity of the displacement characters* $v_{2n+1,2n+2}$. A similar reasoning holds also for the talc structures. The polytypes selected in this way are built on the same symmetry principle (5) and constitute a subfamily (denoted A) of the original family (1). This selection is not only formal because the pairs of OD layers $(L_{3n+1}; L_{3n+2})$ in this subfamily are not geometrically equivalent to the same pairs in the other conceivable subfamily (B) which includes polytypes in whose symbols *all orientational characters are again of the same parity, but this parity is the same as the parity of the displacement characters* $v_{2n+1,2n+2}$. The polytypes belonging to the subfamily B have not yet been encountered [18].

The ditrigonalization does not affect the general form of polytype symbols, it leads merely to an additional parity condition which is different in the two subfamilies. The derivation of MDO polytypes is affected also rather formally. Looking at the packet pairs $(P_1; P_2)$ related by ϱ-operation(s) with reverse continuation it is immediately apparent that, with respect to the additional parity condition, they split into two groups: $\frac{.00.}{3}, \frac{.00.}{1}, \frac{.00.}{5}, \frac{.02.}{1}, \frac{.04.}{5},$ and $\frac{.00.}{0}, \frac{.00.}{2}, \frac{.00.}{4},$ $\frac{.04.}{2}, \frac{.02.}{4}$, leading to the MDO polytypes belonging to the subfamily A or B, respectively. The arrangement in Table III corresponds to this subdivision.

Table IV

The NFZ relations for the pyrophyllite and talc family with ditrigonalized tetrahedràl OD layers

OD layer L_p		Pyrophyllite family layer group	N_p	F	$Z_{p(p-1)}$
L_{3n-1}	(Tet)	$P(3)1m$	6		
				2	
L_{3n}	(Oc)	$P(3)12/m$	6		3
				2	
L_{3n+1}	(Tet)	$P(3)1m$	6		3
				2	
L_{3n+2}	(Tet)	$P(3)1m$	6		3
Talc family					
L_{3n-1}	(Tet)	$P(3)1m$	6		
				6	
L_{3n}	(Oc)	$H(3)12/m$	18		1
				6	
L_{3n+1}	(Tet)	$P(3)1m$	6		3
				2	
L_{3n+2}	(Tet)	$P(3)1m$	6		3

The influence of the ditrigonalization on polytypism in sheet silicates has so far been investigated in the cronstedtite family [27], [28], where it leads to the splitting of this family into four independent subfamilies.

A classification of the MDO polytypes of pyrophyllite and talc as well as the establishing of X-ray identification criteria for them will be the subject of Part II of this contribution.

APPENDIX

The expression(s) in braces in the symbols for some OD groupoid families referring to OD structures consisting of more than one kind of layer, indicate all or almost all ϱ-operations converting a given OD layer into the next one equivalent to it. The classical form of symbols developed by Dornberger-Schiff is very instructive but in some cases redundant and rather complex as e.g. (1) and (5). According to Grell (private communication), they can be simplified using a proposal of Fichtner [29] concerning symbols for OD groupoid families referring to OD structures of equivalent layers. Such symbols give only one of the possible transformations from layer to layer by its rotational part and its translational components referred in case of pyrophyllite and talc families to basic vectors a_3, b_3 (Fig. 3) [30]. The symbols (1) and (5) would then read:

pyrophyllite

$$P(\bar{3})12/m \qquad P(6)mm$$

$$\left[\frac{1}{3}, 0\right] \qquad \left\{(n) \,\middle|\, -\frac{1}{6}, -\frac{1}{6}\right\}$$

instead of (1)

talc

$$H(\bar{3})12/m \qquad P(6)mm$$

$$\left[\frac{1}{3}, 0\right] \qquad \left\{(n) \,\middle|\, -\frac{1}{6}, -\frac{1}{6}\right\}$$

pyrophyllite

$$P(\bar{3})12/m \qquad\qquad P(3)1m$$

$$\left[-\frac{1}{6},\ -\frac{1}{6}\right] \qquad \left\{\bar{1} \left|\ \frac{1}{6},\ -\frac{1}{6}\right.\right\}$$

talc   instead of (5)

$$H(\bar{3})12/m \qquad\qquad P(3)1m$$

$$\left[-\frac{1}{6},\ -\frac{1}{6}\right] \qquad \left\{1 \left|\ \frac{1}{6},\ -\frac{1}{6}\right.\right\}$$

References

[1] Dornberger-Schiff K.: Abh. Dtsch. Akad. Wiss. Berlin Kl. Chem. Geol. Biol. No. 3 (1964).
[2] Dornberger-Schiff K.: *Lehrgang über OD-Strukturen*, Akademie Verlag, Berlin 1966.
[3] Dornberger-Schiff K., Fichtner K.: Krist. Techn. *7*, 1035 (1972).
[4] Dornberger-Schiff K.: Krist. Techn. *14*, 1027 (1979).
[5] Dornberger-Schiff K., Ďurovič S.: Clays Clay Min. *23*, 219 (1975).
[6] Dornberger-Schiff K., Ďurovič S.: Clays Clay Min. *23*, 231 (1975).
[7] Dornberger-Schiff K., Backhaus K.—O., Ďurovič S.: Clays Clay Min. *30*, 364 (1982).
[8] Weiss Z., Ďurovič S.: Acta Cryst. *A36*, 633 (1980).
[9] Ďurovič S., Dornberger—Schiff K., Weiss Z.: Acta Cryst. (submitted).
[10] Weiss Z., Ďurovič S.: Acta Cryst. (submitted).
[11] Gruner J. W.: Z. Kristallogr. *88*, 412 (1934).
[12] Hendricks S. B.: Z. Kristallogr. *99*, 264 (1938).
[13] Stemple I. S., Brindley G. W.: J. Am. Ceram. Soc. *43*, 34 (1960).
[14] Rayner J. H., Brown G.: Clays Clay Min. *13*, 73 (1964).
[15] Ross M., Smith W. L., Ashton W. H.: Am. Mineral. *53*, 751 (1968).
[16] Wardle R., Brindley G. W.: Am. Mineral. *57*, 732 (1972).
[17] Rayner J. H., Brown G.: Clays Clay Min. *21*, 103 (1973).
[18] Zvyagin B. B., Vrublevskaya Z. V., Zhoukhlistov A. P., Sidorenko O. V., Soboleva S. V., Fedotov A. F.: *Vysokovoltnaja elektronografija v issledovanii sloistych mineralov*, p. 62 ff. Nauka, Moskva 1979.
[19] Lee J. H., Guggenheim S.: Am. Mineral. *66*, 350 (1981).
[20] Grell H., Dornberger-Schiff K.: Acta Cryst. *A38*, 49 (1982).
[21] Fichtner K.: Krist. Techn. *14*, 1453 (1979).
[22] Ďurovič S.: Acta Cryst. *B30*, 76 (1974).
[23] Dornberger-Schiff K.: Acta Cryst. *A38*, 483 (1982).
[24] Dornberger-Schiff K., Grell H.: Acta Cryst. *A38*, 491 (1982).
[25] Radoslovich E. W.: Nature (London) *191*, 67 (1961).
[26] Franzini M.: Contr. Mineral. and Petrol. *21*, 203 (1969).
[27] Mikloš D.: CSc. Thesis, Inst. Inorg. Chem. Slovak Acad. Sci., Bratislava 1975.
[28] Mikloš D., Ďurovič S.: Acta Cryst. *A34*, S9 (1978).
[29] Fichtner K.: in *Symposium on special topics of X-ray structure analysis*, Hohengrün DDR, p. 22, Ges. Geol. Wiss DDR 1981.
[30] Grell H.: in *Symposium on special topics of X-ray structure analysis*, Hohengrün DDR, pp. 18—21, Ges. Geol. Wiss. DDR 1981.

POLYTYPIZMUS PYROFYLITU A MASTENCA
ČASŤ I. OD INTERPRETÁCIA A MDO POLYTYPY

Slavomil Ďurovič, Zdeněk Weiss*)

Ústav anorganickej chémie, Centrum chemického výskumu, Slovenská akadémia vied, 842 36 Bratislava
*)*Vědeckovýzkumný uhelný ústav, 716 07 Ostrava-Radvanice*

Polytypické štruktúry pyrofylitu a mastenca s idealizovanou symetriou ich tetraedrických vrstiev sú OD štruktúry pozostávajúce z dvoch druhov vrstiev a patria do kategórie I. Týmto sa vysvetľuje polytypizmus týchto minerálov a umožňuje odvodenie ich štandardných (MDO)

16

polytypov, ktoré sú potrebné pre stanovenie identifikačných kritérií. Spolu existuje 30 nekongruentných (22 neekvivalentných) MDO polytypov v pyrofylitovej famílii a 12 (10) MDO polytypov v mastencovej famílii. Ideálna ditrigonalizácia tetraedrických vrstiev nemení počet MDO polytypov, avšak obmedzuje možnosti nakladania jednotlivých OD vrstiev a spôsobuje rozdelenie polytypov do dvoch kryštalochemicky nezávislých subfamílií v rámci príslušnej pyrofylitovej resp. mastencovej famílie. Jednotlivé polytypy sú charakterizované úplnými symbolmi, ktoré sú v súlade s jednotnou symbolikou polytypov vrstevnatých silikátov.

Obr. 1. Schéma kryštálových štruktúr pyrofylitu a mastenca. Ukázané sú OD vrstvy, OD pakety, ich označenie a polarita.

Obr. 2. Posunové vektory ⟨v⟩, ich vzťah k základným vektorom a_1, a_2 a ich konvenčné charaktery:

$$\langle 0\rangle = (-1/3, -1/3); \quad \langle 1\rangle = (-1/3, 0); \quad \langle 2\rangle = (0, 1/3);$$
$$\langle 3\rangle = (1/3, 1/3); \quad \langle 4\rangle = (1/3, 0); \quad \langle 5\rangle = (0, -1/3);$$
$$\langle *\rangle = (0, 0); \quad \langle +\rangle = (-1/3, 1/3); \quad \langle -\rangle = (1/3, -1/3).$$

Obr. 3. Osový systém použitý v tejto práci. $|b_i| = |a_i|/\sqrt{3}$

Obr. 4. Sekvencia piatich OD vrstiev (vľavo) a zodpovedajúca sekvencia v štyroch OD paketov (vpravo) v štruktúre pyrofylitu (a) a mastenca (b). OD vrstvy a OD pakety sú číslované podľa ich poradia, L_m/L_n znamená koincidenciu týchto vrstiev v X_1, X_2 projekcii. Posunové vektory ⟨v⟩ sú charakterizované v súlade s obr. 2.

Obr. 5. Štyri typické páry súsediacich pyrofylitových OD paketov (P_0; P_1) (a, c) a (P_1; P_2) (b, d) spolu s im zodpovedajúcimi symbolmi. Osobitne sú zdôraznené príslušné ϱ- koincidenčné operácie a ich povaha (prítomnosť alebo neprítomnosť spätného pokračovania). OD pakety sú číslované podľa ich poradia.

Obr. 6. Schematické zobrazenie pyrofylitového (a) a mastencového polytypu (b) OD pakety sú číslované podľa ich poradia; posunové vektory, symboly polytypov a ich priestorové grupy sú tiež uvedené.

ПОЛИТИПИЯ ПИРОФИЛЛИТА И ТАЛЬКА
1. ОД ИНТЕРПРЕТАЦИЯ И МДО ПОЛИТИПЫ

Славомил Дюрович, Зденек Вейсс*)

*Институт неорганической химии, база химического исследования
Словацкая Академия Наук, 842 36 Братислава*
*) *Научно-исследовательский институт угля, 716 07 Острава-Радванице*

Политипические структуры пирофиллита и талька с идеализированной симметрией их тетраэдрических слоев представляют собой ОД структуры, состоящие из двух видов слоев и относятся к категории 1. Тем объясняется политипия данных минералов, и возникает возможность выведения их стандартных (МДО) политипов, необходимых для установления идентификационных критериев. Сосуществует 30 неконгруентных (22 неэквивалентных) МДО политипов в пирофиллитовом семействе и 12 (10) МДО политипов в семействе талька. Идеальная дитригонализация тетраэдрических слоев не изменяет количество МДО политипов, однако ограничивает возможности комбинации отдельных ОД слоев и вызывает разделение политипов в два кристаллохимически независимые субсемейства в рамках соответствующего семейства пирофиллита или талька. Отдельные типы характеризуются полными символами, которые находятся в согласии с отдельным символизмом политипов слоистых силикатов.

Рис. 1. Схема кристаллических структур пирофиллита и талька. Показываются ОД слои, ОД пакеты, их обозначение и полярность.

Рис. 2. Векторы смешения ⟨v⟩, их отношение к осносным векторам a_1, a_2 и их условные характеры:

$$\langle 0\rangle = (-1/3, -1/3); \quad \langle 1\rangle = (-1/3, 0); \quad \langle 2\rangle = (0, 1/3); \quad \langle 3\rangle = (1/3, 1/3);$$
$$\langle 4\rangle = (1/3, 0); \quad \langle 5\rangle = (0, -1/3), \quad \langle *\rangle = (0, 0); \quad \langle +\rangle = (-1/3, 1/3);$$
$$\langle -\rangle = (1/3, -1/3).$$

Рис. 3. Координатная система, применяемая в работе: $|b_i| = |a_i|/\sqrt{3}$

Рис. 4. Последовательность пяти ОД слоев (налево) и соответствующая последовательность четырех ОД пакетов (направо) в структуре пирофиллита (а) и талька (b). ОД слои и ОД пакеты обозначены номерами согласно их порядку, L_m/L_n

обозначает совпадение данных слоев в X_1, X_2 проекции. Векторы смещения $\langle v \rangle$ характеризуются согласно рис. 2.

Рис. 5. *Четыре типичные пары смежных пирофиллитовых ОД пакетов (P_0; P_1) (a, c) и (P_1; P_2) (b, d) вместе с им соответствующими символами. Особенно подчеркиваются соответствующие ρ-операции совпадения и их характер (присутствие или отсутствие реверсного продолжения). ОД пакеты обозначены номерами согласно их порядку.*

Рис. 6. *Схематическое изображение политипа пирофиллита (a) и талька (b). ОД пакеты обозначены номерами согласно их порядку; векторы смещения, символы политипов и пространственные группы также приводятся.*

FELIX TROJER, KARL-HEINZ OBST, WOLFGANG MÜNCHBERG: MINERALOGIE BASISCHER FEUERFEST — PRODUKTE (Mineralogie bázických žárovzdornin). Springer—Verlag, Wien, New York 1981. 180 str., 191 obr., cena 98 DM.

Kniha je 12. svazkem v řadě „Technická mineralogie". Autoři působí v současnosti na universitách v Leobenu, Clausthalu a Freiburgu, po předchozí výzkumné činnosti v laboratořích předních výrobců bázických žárovzdornin, a jsou uznávanými odborníky v oblasti technické mineralogie. Pojetí knihy je vhodně zvoleno v souladu se současným zaměřením mineralogie technických materiálů, tzn. s důrazem na výklad vztahu mezi fázovým složením, strukturou a texturou materiálu a jeho fyzikálními a technickými vlastnostmi. K tomu je nutno na jedné straně komplexně využít všechny diagnostické metody (optickou a elektronovou mikroskopii, RTG-mikroanalýzu a RTG-difrakci, DTA, IČ spektroskopii a chem. analýzu). Na druhé straně je nezbytné začlenit poznatky o mineralogickém složení materiálů do fyzikálně chemického výkladu a dosáhnout tak vysvětlení příčin procesů, které vedly ke vzniku fázového složení a struktury jak nepoužitých žárovzdornin, tak po jejich aplikaci v průmyslových pecích. Tento záměr se autorům v podstatě podařil. Přispělo k tomu i vhodné členění knihy, v jejímž úvodu je čtenář informativně seznámen s metodami technické mineralogie. Určitým nedostatkem jsou nevyvážené odkazy na podrobnější literaturu k jednotlivým metodám — např. k rentgenové difrakci je uveden jediný pramen, a to z roku 1961. Speciální část knihy má 4 kapitoly. V první se pojednává o mineralogii surovin, s uvedením typických příkladů složení a struktur. Druhá kapitola je zaměřena na meziprodukty: slínky vyrobené z magnezitu, dolomitu a kalcitu a odpovídající tavené produkty včetně taveného materiálu na bázi periklasu a chromspinelu. Důsledně je diskutován zejména vztah chem. složení suroviny a teploty výpalu k fázovému složení produktu. Další kapitola pojednává o mineralogii produktů, pálených i nepálených. Jsou uváděny konkrétní příklady jednotlivých typů bázických žárovzdornin, jejich struktur, a difraktogramů. Značná pozornost je věnována výkladu změn fázového složení a struktury materiálů po jejich použití. S ohledem na převládající aplikaci je kapitola 4 zaměřena především na změny vyvolané hutnickými produkty, zejména struskou. V závěru této kapitoly je pojednáno i o změnách po aplikaci v cementářských a vápenických pecích, v pecích na výpal magnezitového slínku a v regenerátorech sklářských pecí (zde relativně stručně a se skromným literárním odkazem).

Závěrem lze shrnout, že kniha představuje zasvěcený úvod — a to je dáno jejím rozsahem — do mineralogie bázických žárovzdornin. Nespornou předností je moderní pojetí technické mineralogie, shrnutí původních prací z periodické literatury do monografie, dobrá odborná úroveň zpracování i kvalita reprodukcí a tisku. Více pozornosti mohlo být věnováno určování fázového složení (včetně sekundárních produktů po aplikaci) rentgenograficky. Čtenář by jistě uvítal i tabelární shrnutí základních optických a spektrálních dat i přehled difrakcí jednotlivých fází. Kniha najde své zájemce mezi výzkumnými pracovníky v oblasti bázických žárovzdornin a bude užitečnou pomůckou i technickým mineralogům.

M. Bartuška

.